J. Phys. B: At. Mol. Opt. Phys. **33** (2000) 3531–3544. Printed in the UK PII: S0953-4075(00)50536-7

Elastic electron scattering from sulfur hexafluoride

H Cho†, R J Gulley, K W Trantham‡, L J Uhlmann, C J Dedman and S J Buckman

Atomic and Molecular Physics Laboratories, Research School of Physical Sciences and Engineering, Australian National University, Canberra, ACT 0200, Australia

Received 11 April 2000, in final form 22 June 2000

Abstract. Absolute differential cross sections for elastic scattering of electrons from sulfur hexafluoride (SF_6) have been measured at 11 incident energies between 2.7 and 75 eV and for scattering angles between 10° and 130°. The magnetic angle-changing device of Read and co-workers has been used to extend these measurements to backward angles (130°–180°) for incident energies below 15 eV. The measurements reveal some substantial differences with several previous determinations and a reasonably good level of agreement with a recent close-coupling calculation.

(Some figures in this article are in colour only in the electronic version; see `www.iop.org`)

1. Introduction

The interaction of low-energy electrons with sulfur hexafluoride (SF_6) has been the subject of numerous experimental and theoretical studies due to its involvement in plasma discharge processes and as the most commonly used insulating gas in the electrical industry. Since SF_6 has a very large cross section for near-threshold attachment (Christophorou and van Brunt 1995), low-energy electrons are readily scavenged, principally to form SF_6^-, before they have the chance to generate an avalanche breakdown. To better achieve understanding and control in these applications, plasma modelling and electron transport equations require an extensive range of electron-impact cross section data including the elastic cross section. It has recently been noted (Hayashi and Nimura 1984, Christophorou *et al* 1999) that the measured total cross sections for electron scattering from SF_6 at energies between about 5 and 100 eV are inconsistent with the sum of total elastic and inelastic cross sections in this energy region. Furthermore, the elastic differential cross sections, from which the total elastic values have been derived, also demonstrate inconsistencies in this energy range.

There have been many experimental investigations of electron–SF_6 interactions over the past two decades. Srivastava *et al* (1976) measured the elastic differential cross section (DCS) at electron impact energies from 5 to 75 eV. They applied the relative flow technique (Srivastava *et al* 1975, Nickel *et al* 1989), using the helium differential cross section of McConkey and Preston (1975) as the reference cross section. These measurements were subsequently renormalized using the improved helium cross section of Register *et al* (1980) and reported in the review paper of Trajmar *et al* (1983). Rohr (1979) measured the energy dependence of the elastic DCS at energies from 0.05 to 10 eV and for scattering angles between 10° and 120°, and the angular dependence at a few selected energies. His relative cross section measurements

† Permanent address: Physics Department, Chungnam National University, Taejon, Korea.
‡ Present address: Department of Physical and Life Sciences, Arkansas Technical University, AR 72801, USA.

0953-4075/00/183531+14$30.00

were placed on an absolute scale by comparing the SF_6 scattering rates with those of helium, but the helium cross section that was used for this purpose was not specified. Sakae *et al* (1989) reported elastic DCS for the higher energy range of 75 to 700 eV and the angular range of 5°–135°. Their cross sections were placed on an absolute scale by measuring relative scattering intensities for SF_6 and He in their scattering chamber at an angle of 30°. The He cross sections of Jansen *et al* (1976) and Register *et al* (1980) were used in this process. Johnstone and Newell (1991) presented the elastic DCS for incident energies between 5 and 75 eV and for scattering angles in the range 10°–120°. They normalized their relative measurements at a scattering angle of 90° to the helium cross section of Nesbet (1979), at energies below 20 eV, and to that of Register *et al* (1980) at higher energies. They used the relative flow technique for this process. The energy dependence of both the elastic cross section and that for vibrational excitation were studied by Trajmar and Chutjian (1977) but absolute values were not measured.

Kennerly *et al* (1979) report the absolute grand total cross section for incident electron energies between 0.5 and 100 eV obtained by two independent experimental techniques. Dababneh *et al* (1988) measured the total cross section for electron scattering as well as positron scattering from SF_6 over the incident energy range of 1–500 eV using a beam-transmission technique. Other total cross section measurements reported in the energy region of the present results are those of Ferch *et al* (1982), Zecca *et al* (1992) and Kasperski *et al* (1997).

On the theoretical side there has been substantially less contemporary activity. Gianturco *et al* (1995) calculated elastic DCS over an energy range 3.3–30 eV by solving the multichannel scattering problem within the close-coupling approach. Dehmer *et al* (1978) and Gyemant *et al* (1980) have also done some theoretical work on SF_6, mainly concerned with the resonance structures in electron scattering. Jiang *et al* (1995, 1997) have reported both DCS (100–700 eV) and TCS (10–1000 eV) for electron scattering from SF_6.

SF_6 is a non-polar molecule but it has a high dipole polarizability of 44 au. It also possesses many low-energy shape resonances which have been extensively studied both experimentally and theoretically (for example, Dehmer *et al* 1978, Kennerly *et al* 1979, Dababneh *et al* 1988, Kaspersky *et al* 1997, Gianturco *et al* 1995). The positions (energies) of these resonances vary slightly from one result to the other but in summary they are believed to be the a_{1g}, t_{1u}, t_{2g} and e_g resonances appearing at around 2.7, 7, 12 and 27 eV, respectively (Dehmer *et al* 1978, Gianturco *et al* 1995). These calculations have also revealed the likely partial waves in which the resonances occur and differential measurements provide us with the ability to test these predictions. Also, a substantial increase in the total scattering cross section below 1 eV is dominated by electron attachment at near zero energies. Indeed, measurements of the attachment rate and cross section at low energies have been the subject of a large amount of recent work.

In this paper we present absolute measurements of the differential cross section for elastic scattering from SF_6 at 11 incident energies between 2.7 and 75 eV and for scattering angles in the range 10°–180°. A version of the magnetic angle-changing device developed by Read and Channing (1996) has been successfully applied with the relative flow technique to measure the DCS at backward scattering angles up to 180°, where cross section measurements are typically inaccessible due to the mechanical constraints of an electron spectrometer. Part of the motivation for these measurements was a discrepancy in the published total elastic cross sections (Christophorou *et al* 1999), the elastic DCS have been extrapolated and integrated to derive total elastic and momentum transfer cross sections. These have been reported and discussed in a recent communication (Cho *et al* 2000), along with examples of the elastic DCS at 5 and 75 eV.

2. Experimental considerations

2.1. Electron spectrometer and relative flow technique

The present experiments were carried out using a conventional crossed electron–molecular beam spectrometer. This apparatus has been described in detail previously (Brunger *et al* 1990, Gulley *et al* 1994). It is capable of differential scattering measurements over an angular range from -20° and 130° about the molecular beam axis. In the present case a magnetic angle-changing device, similar to that developed by Read and co-workers (Read and Channing 1996, Zubek *et al* 1996, 1999), has been used to measure the differential cross sections at angles between 130° and 180°. This important addition to the experimental apparatus is described in the next section. The molecular beam is formed by quasi-effusive flow of SF_6 through a multicapillary array. This beam is then crossed with an electron beam, produced by a combination of a thoriated tungsten filament, electrostatic electron optical elements and a hemispherical monochromator. Scattered electrons, either elastic or inelastic, are energy analysed and detected by a further combination of electron optical elements, a hemispherical analyser and a channel electron multiplier. The overall energy resolution of the spectrometer for these measurements was typically 50–60 meV and the electron beam current in the interaction region ranged from 0.8 to 3 nA, depending somewhat on the incident energy.

The absolute electron energy scale is calibrated by observing either the position of the second quasi-vibrational resonance peak of the $N_2^-\ ^2\Pi_g$ resonance at an energy of 2.198 eV for a scattering angle of 60° (Rohr 1977), or the position of the $He^-\ 1s2s^2\ ^2S$ resonance at 19.367 eV (Brunt *et al* 1977). The absolute cross sections at each energy and scattering angle were determined by use of the relative flow technique. This technique relies on measurements of the ratio of scattered electron intensities for the gas of interest relative to that for a standard gas. The commonly used standard cross section is that of helium. For the present angular differential measurements, we have used the elastic differential cross sections of Nesbet (1979) for energies below 20 eV. At higher energies we have used the helium elastic scattering cross sections measured in this laboratory by Brunger *et al* (1992) and convergent close-coupling calculation by Fursa and Bray (1997) as the reference cross sections.

A number of important conditions need to be fulfilled to properly conduct a relative flow experiment. These have been have been discussed in some detail by Nickel *et al* (1989), Buckman *et al* (1993), Gibson *et al* (1999) and references therein, and we shall not dwell on them further. One of the most important aspects, however, is the need to ensure that the interaction volume is the same size for each gas. The first step in this process is to ensure that the mean free paths of the two gases in the beam-forming device are the same. The mean free paths are calculated from values of the hard-sphere diameters for each of the gases. For SF_6 the values found in the literature vary between $\sigma = 6.047$ Å (calculated from tabulated values of Reid *et al* (1987)) and $\sigma = 6.35$ Å (Wilhelm and Battino 1971). We have used a value $\sigma = 6.2$ Å and, in conjunction with the value for helium ($\sigma = 2.19$ Å, Landolt-Börnstein 1971), this results in a driving pressure ratio (He/SF_6) of about 8. The effect that gas cycling has on contact potential differences and the stability of the electron optical elements has been minimized by having both gases present in the scattering chamber at all times. This is achieved by having two gas inlets, one to the interaction volume and the other via a capillary on the periphery of the scattering chamber. When one gas flows to the interaction region the other is routed to the peripheral inlet and vice versa. Background contributions are measured at each angle by flowing both gases to the peripheral input. All aspects of the gas routing and data acquisition are computer controlled.

The measurements of the energy dependence of the elastic differential cross section have been obtained using a technique which has been previously described in some detail (Gibson *et al* 1996). It involves sequential measurements of the energy dependence of the elastic scattering rates for SF_6, He and the background gas, together with measurements of the energy dependence of the electron beam current and measurements of gas driving pressures. During the energy scanning process, the zoom lenses in both the monochromator and analyser were also scanned to maintain the focal properties of the electron beam and the transmission characteristics of the energy analyser. However, the final absolute values for the energy dependence of the SF_6 cross section do not depend on a detailed knowledge of the transmission characteristics of the spectrometer as the data are placed on an absolute scale, at each individual energy and scattering angle, by reference to the He elastic scattering cross sections of Nesbet and by use of the relative flow technique.

2.2. Magnetic angle-changing device

To enable measurements at angles beyond the upper mechanical limit imposed by the physical size of the electron source and the analyser/detector ($\sim 130^\circ$ in our case), the novel magnetic angle-changing technique of Read and Channing (1996) has been utilized. They demonstrated that the scattering geometry of an apparatus could effectively be rotated, with respect to the position of the monochromator/analyser, by surrounding the interaction volume by two pairs of magnetic field coils producing opposed, but coaxial, magnetic fields. The use of two concentric coils ensures that the electron beam always passes through the common centre of the coils and, furthermore, if the coils are carefully positioned and the coil currents are delicately balanced, the magnetic field that is produced can be highly localized and symmetric about the axis of the molecular beam. In this way the incident beam can be deflected through an arbitrarily large angle in the scattering plane. The scattered electrons are also deflected as they emerge from the interaction volume and, if there is no energy loss during the collision, they will suffer the same angular rotation as the incident beam. For example, deflection of the incident beam by an angle of 45° results in the unscattered or elastically scattered electrons undergoing a similar, additional rotation as they exit the field. Thus the incident beam emerges from the region of the B-field at an angle of 90° to the original direction and the scattering geometry is effectively rotated by 90°. As a result an electron analyser placed at the conventional 90° position will record elastic electron scattering events occurring at a 'real' angle of 180°. This technique has been successfully used in a number of recent applications (Zubek *et al* 1996, 1999, Trantham *et al* 1997, Allan 2000, Cho *et al* 2000) and further details of its general application can be found in these papers.

The principal design criteria for these devices have been discussed by Read and Channing (1996). In a small departure from their design, we have used high permeability (μ-metal) pole pieces, together with a unique coil arrangement, to further minimize external stray magnetic fields. Our design, shown schematically in figure 1, is based on a 'magnetic circuit' where the arrangement of the pole pieces and coils (and their currents) are such that the outer surfaces of the device are at the same magnetic 'potential'. The device has been extensively computer modelled (Trantham *et al* 1997), with the prediction that stray magnetic fields at a distance 10 cm from the outside edge of the pole pieces can be as much as seven orders of magnitude less than that inside and between the magnets (i.e. in the scattering plane). The stray flux generated by the magnet device has been tested by the use of a fluxgate magnetometer (Schonstedt DM2200) with a resolution of 10^{-9} T. At a distance of 10 cm from the coil axis, the stray field from the coil pair was about 5×10^{-8} T when the outer (larger) coil current was set to 1.2 A, corresponding to a $\boldsymbol{B}$ field of about 3×10^{-3} T—sufficient to rotate the scattering

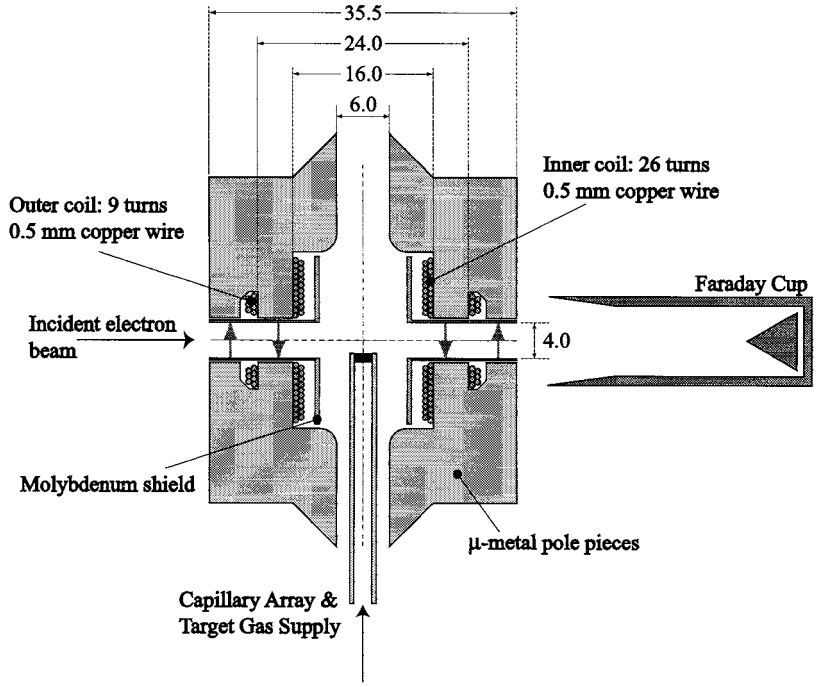

Figure 1. A schematic diagram of the magnetic angle-changing device. The dimensions shown are in millimetres. The arrows indicate the direction of the $\boldsymbol{B}$ fields within the pole pieces.

plane by 90° at an incident energy of 15 eV. In practice we also have a very sensitive, *in situ* magnetometer in the form of the electron monochromator where the electron beam is energy analysed, typically at a pass energy of 1.5 eV. The central path of the monochromator is located about 15 cm from the coil centre and there is no measurable change in the transmitted current when the coils are activated. Indeed, the largest source of stray flux due to the use of the device is from the vacuum/electrical feedthrough where the current carrying wires are connected and it is difficult to achieve completely non-inductive winding.

As the device is self-shielding we have also observed that the operation of the electron spectrometer is also relatively insensitive to small changes in the ratio of the inner coil current to the outer coil current. This is an advantage over an 'open-area' coil arrangement which, as previously noted, relies on a sensitive balance of the inner and outer coil currents to minimize external fields. The only disadvantage that we have noted with the present design is an increase in background scattering at low energies, presumably due to the proximity of the surfaces of the pole pieces. This, however, has not proved to be a major concern and could most likely be improved by small design changes. In the present series of measurements we have used the coils to rotate the scattering geometry through 90°. Two Faraday cups are used to monitor the electron beam current. It was also noted that all of the current which was incident on the Faraday cup placed at the traditional 0° position could be collected in a similar cup placed at 90° when the $\boldsymbol{B}$ fields were turned on.

Measurements of the differential cross section using this device have been performed for incident electron energies up to and including 15 eV. Thermal limitations on the enamelled wire used for the field coils in the present device precluded safe operation above this energy if the

scattering geometry is rotated through an effective angle of 90° as described above. However, given the substantial thermal mass of the pole pieces, and reasonably efficient heatsinking via large Macor mounts, it should be possible to operate the device at substantially higher energies with appropriately insulated wire.

3. Results and discussion

3.1. Elastic differential cross sections

Absolute, elastic differential cross sections have been measured at 11 different energies ranging from 2.7 to 75 eV, including measurements at several energies which correspond to the positions of negative ion resonances. These data are presented in table 1 and examples of the DCS and comparison with previous results are provided in figures 2–4. The experimental uncertainties on each measured point are indicated in the table as a percentage. They arise from a combination (in quadrature) of the statistical uncertainties (1–10%) together with those arising from measurements of parameters such as electron current (2%), gas pressure and the determination of relative flow rates (5%) and the helium cross section (5%). The overall absolute uncertainties in the tabulated differential cross sections are thus typically less than 10%. For the energy dependence measurements, the statistical accuracy is usually not as high as for the angular DCS data, and the absolute uncertainties are estimated to lie in the 15–20% range.

The energies at which negative ion resonances occur in electron scattering from SF_6 have been determined in a number of previous measurements (e.g. Rohr 1979, Kennerly *et al* 1979). In the present case we have extended the measurements of Rohr, on the energy dependence of the elastic DCS, to the energy region above 6 eV, in order to establish those energies at which the present DCS measurements might further our understanding of these resonances. These absolute excitation functions, obtained using the relative flow technique, are shown in figure 2 at scattering angles of 60°, 90° and 120°. Where there is overlap with the absolute measurements of Rohr (at 60° and 120°) the agreement is reasonable, both with regard to the positions of the features and the absolute magnitude of the cross sections. A resonance is clearly visible in the present data at an energy 12 eV and less prominent at an energy around 6–7 eV. Although they are not shown here, the present measurements also show good agreement with the relative measurements of Trajmar and Chutjian (1977). They were the first to identify the strong resonance at 12 eV, although they did not speculate as to its classification. Also shown on these figures are the results of the conventional DCS measurements at several discrete energies and it can be seen that there is generally good accord between the two different techniques.

At an incident electron energy of 2.7 eV (the position of the a_{1g} resonance) the elastic DCS is relatively small in magnitude at all scattering angles and the angular dependence indicates a turnover (decrease) in the cross section at angles below about 40° and a minimum at 95°, as shown in figure 3(*a*). At backward angles the cross section increases smoothly to a value at 180° of about 1.5 $Å^2$ sr^{-1}. The present result compares favourably with the measurements of Rohr (1979) at most scattering angles. Dehmer *et al* (1978) have found that the partial waves giving the biggest contribution to the cross section at this energy are $l = 0$ and 4, with the latter being the dominant contributor. This is not inconsistent with the observation in figure 3(*a*). However, one must be cautious as it is often more difficult to determine the dominant partial waves for a resonance in the elastic channel (than for vibrational excitation for instance) due to the interference which occurs with the substantial direct scattering amplitudes. In the case of SF_6 this has also been amplified by Gianturco *et al* (1995) who believe that the observed

Table 1. Differential cross sections for elastic electron scattering (in units of 10^{-16} cm^2 sr^{-1}) and total elastic and elastic momentum transfer cross sections, σ_i and σ_m, respectively (in units of 10^{-16} cm^2) from SF_6. Values in parentheses indicate estimated percentage uncertainties and the estimated uncertainty on the integral and momentum transfer cross sections is ±20%.

Angle	Energy (eV)				
(deg)	2.7	5.0	7.0	8.5	10
15			5.896(8)	8.500(11)	11.168(7)
20	1.949(13)	3.939(11)	7.899(7)	8.823(9)	8.892(7)
25	1.990(8)	4.225(7)	6.843(7)	7.720(7)	7.558(8)
30	2.336(7)	4.001(8)	5.899(7)	6.404(7)	6.236(7)
35	2.467(7)	3.827(8)	4.893(7)	5.201(8)	4.811(7)
40	2.516(8)	3.597(7)	3.988(7)	3.893(7)	3.507(7)
45	2.506(8)	3.143(8)	2.995(7)	2.811(7)	2.517(7)
50	2.401(8)	2.819(9)	2.201(7)	2.066(7)	1.708(8)
55	2.184(8)	2.329(7)	1.550(7)	1.442(7)	1.189(7)
60	2.049(7)	1.894(7)	1.107(7)	1.089(7)	1.028(7)
65	1.787(7)	1.422(8)	0.873(7)	0.953(7)	0.982(7)
70	1.539(7)	1.150(7)	0.802(7)	0.941(7)	1.091(8)
75	1.405(7)	0.907(9)	0.842(7)	1.073(7)	1.263(7)
80	1.199(7)	0.825(8)	1.002(7)	1.263(7)	1.456(9)
85	1.077(8)	0.795(7)	1.153(7)	1.317(8)	1.531(8)
90	0.969(8)	0.884(8)	1.288(7)	1.391(8)	1.516(9)
95	0.906(8)	0.960(9)	1.388(7)	1.385(7)	1.413(12)
100	0.935(8)	1.124(8)	1.420(7)	1.345(7)	1.244(8)
105	0.981(8)	1.229(7)	1.397(7)	1.217(7)	1.067(8)
110	1.037(7)	1.268(9)	1.296(7)	1.069(8)	0.952(7)
115	1.057(7)	1.254(8)	1.165(8)	0.945(7)	0.831(7)
120	1.099(8)	1.231(9)	1.048(7)	0.816(7)	0.771(8)
125	1.236(7)	1.150(11)	0.909(7)	0.745(7)	0.779(7)
130	1.311(7)	1.016(9)	0.810(7)	0.830(12)	0.846(8)
135	1.351(7)	0.956(8)	0.977(7)	0.956(7)	0.916(7)
140	1.372(7)	0.908(8)	0.999(7)	0.995(7)	0.999(8)
145	1.402(8)	0.792(8)	1.006(7)	1.072(8)	1.113(7)
150	1.415(7)	0.744(9)	1.110(7)	1.233(7)	1.173(7)
155	1.390(7)	0.703(8)	1.235(7)	1.305(8)	1.247(7)
160	1.485(7)	0.641(7)	1.288(7)	1.467(8)	1.306(7)
165	1.486(7)	0.606(7)	1.395(8)	1.571(9)	1.357(7)
170	1.485(7)	0.576(8)	1.467(7)	1.618(8)	1.369(7)
175	1.499(7)	0.572(7)	1.512(7)	1.706(7)	1.440(7)
180	1.500(7)	0.535(9)	1.542(7)	1.775(7)	1.473(8)
σ_i	18.73	20.15	24.29	24.60	24.45
σ_m	16.10	14.14	15.47	14.49	15.09

structure in the elastic DCS is, in fact, dominated by direct scattering processes. The theoretical curve which is shown in this figure is the calculation of Gianturco *et al* (1995), but at an energy of 3.3 eV—the energy at which the calculation predicts the presence of the a_{1g} resonance. There is little accord between the theoretical and the two experimental cross sections, either in shape or absolute magnitude. This is yet another example of how resonance positions in fixed-nuclei computations appear to be shifted to higher collision energies when compared with experimental measurements because of the explicit neglect of nuclear motion (Gianturco *et al* 1995).

Table 1. Continued.

Angle (deg)	Energy (eV)					
	12	15	20	30	50	75
10	13.788(17)		23.711(8)	55.574(8)	49.457(7)	45.477(8)
15	15.218(8)	12.994(7)	15.656(7)	23.329(7)	24.678(7)	15.422(8)
20	12.415(7)	11.128(7)	10.983(9)	13.255(7)	9.672(8)	4.414(9)
25	9.312(7)	8.699(7)	7.988(7)	6.916(7)	3.510(8)	1.369(13)
30	6.651(7)	6.652(7)	5.246(8)	3.307(7)	1.606(8)	1.230(8)
35	4.511(7)	4.649(7)	3.228(10)	1.573(7)	1.295(8)	1.379(10)
40	2.911(8)	3.046(7)	1.867(7)	0.988(7)	1.376(8)	1.326(10)
45	1.724(7)	1.837(7)	1.002(9)	0.993(7)	1.378(7)	0.965(8)
50	1.104(7)	1.126(7)	0.703(9)	1.266(7)	1.159(10)	0.670(8)
55	0.748(7)	0.839(7)	0.740(9)	1.369(7)	1.038(8)	0.478(8)
60	0.677(8)	0.869(7)	0.984(9)	1.430(7)	0.758(10)	0.340(8)
65	0.737(8)	1.053(7)	1.331(11)		0.533(11)	0.298(8)
70	0.858(8)	1.246(7)	1.433(10)	1.052(8)	0.342(9)	0.274(10)
75	0.994(8)	1.393(7)	1.500(8)		0.236(9)	0.262(10)
80	1.088(8)	1.403(7)	1.343(7)	0.655(8)	0.180(12)	0.248(12)
85	1.103(8)	1.308(7)	1.128(8)		0.199(9)	0.231(9)
90	1.168(7)	1.218(7)	1.011(8)	0.402(7)	0.234(9)	0.214(11)
95	1.193(8)	1.069(7)	0.823(9)		0.283(8)	0.218(14)
100	1.132(8)	0.974(8)	0.690(7)	0.473(7)	0.316(9)	0.194(8)
105	1.095(7)	0.864(7)	0.596(8)		0.320(10)	0.182(9)
110	1.117(7)	0.791(7)	0.611(8)	0.643(8)	0.348(10)	0.210(10)
115	1.210(8)	0.778(7)	0.602(8)		0.389(11)	0.262(13)
120	1.376(8)	0.765(7)	0.669(8)	0.873(7)	0.420(10)	0.356(10)
125	1.450(7)	0.811(7)	0.811(9)		0.469(11)	0.472(11)
130	1.544(7)	0.867(7)	0.933(7)	1.098(7)	0.583(12)	0.632(13)
135	1.566(7)	0.971(7)				
140	1.616(7)	1.118(7)				
145	1.651(7)	1.257(7)				
150	1.686(7)	1.353(7)				
155	1.711(7)	1.495(8)				
160	1.758(7)	1.652(7)				
165	1.752(8)	1.774(7)				
170	1.829(8)	1.915(7)				
175	1.862(7)	1.940(7)				
180	1.843(7)	1.973(7)				
σ_i	26.81	25.51	24.73	29.72	22.13	18.02
σ_m	17.62	14.86	15.65	13.18	8.09	7.28

At 5 eV (figure 3(*b*)) the present DCS is once again consistent with that of Rohr at all scattering angles. The local maximum at forward scattering angles has moved to smaller angles ($\sim 25^\circ$) as has the local minimum at backward angles which has moved to about 85°. The cross section decreases at forward scattering angles ($< 25^\circ$), an interesting trend given the large dipole polarizability of the molecule. It is interesting to note that the use of the magnetic angle-changing device enables us to determine that the smallest value of the cross section actually occurs for backscattering (180°). At this energy, and above, there are also the experimental results reported by Srivastava *et al* (1976) and Johnstone and Newell (1991). However, the level of agreement with both of these results, which agree rather well with each other, and the present cross section is rather poor, particularly at more forward scattering angles. Here, the

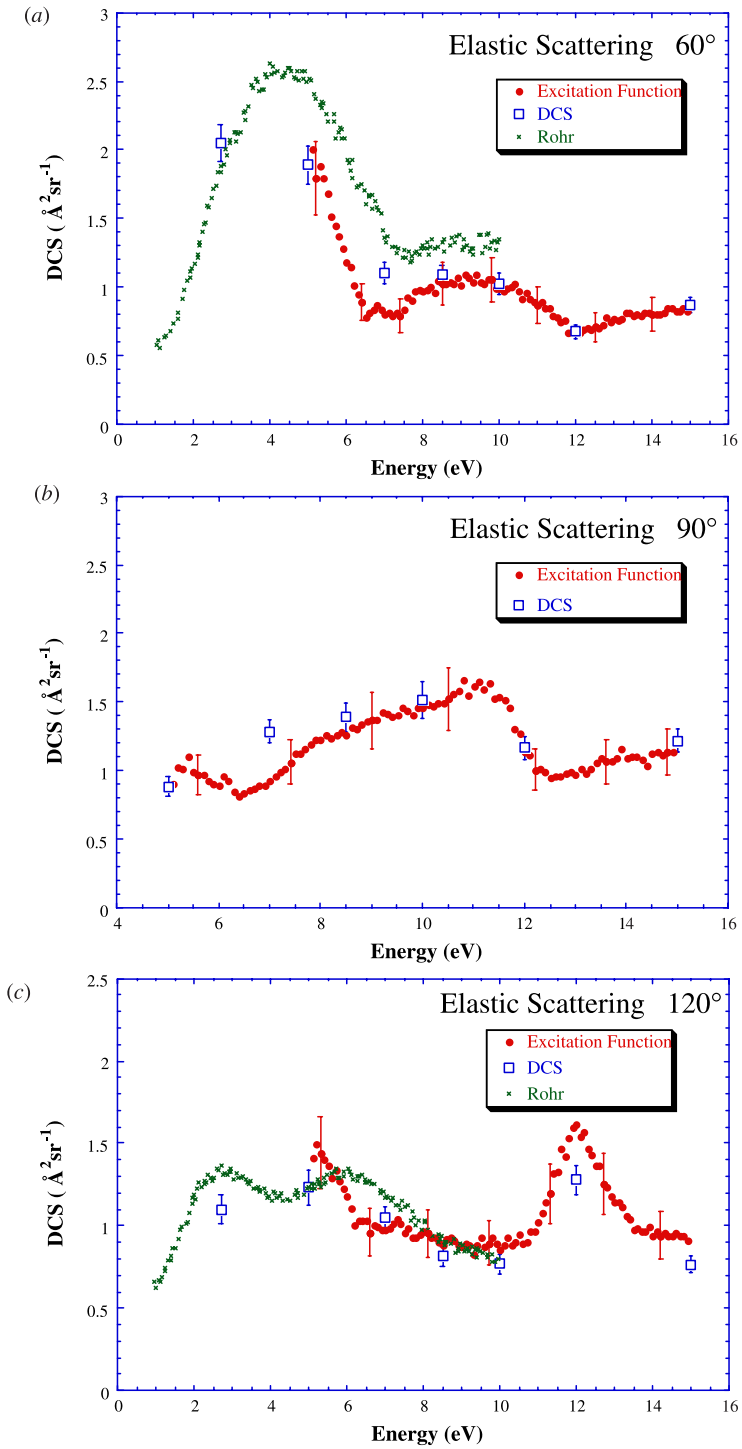

Figure 2. Elastic excitation function at a scattering angle of (*a*) 60°, (*b*) 90°, (*c*) 120°: ●, present excitation function; □, present DCS; ×, Rohr.

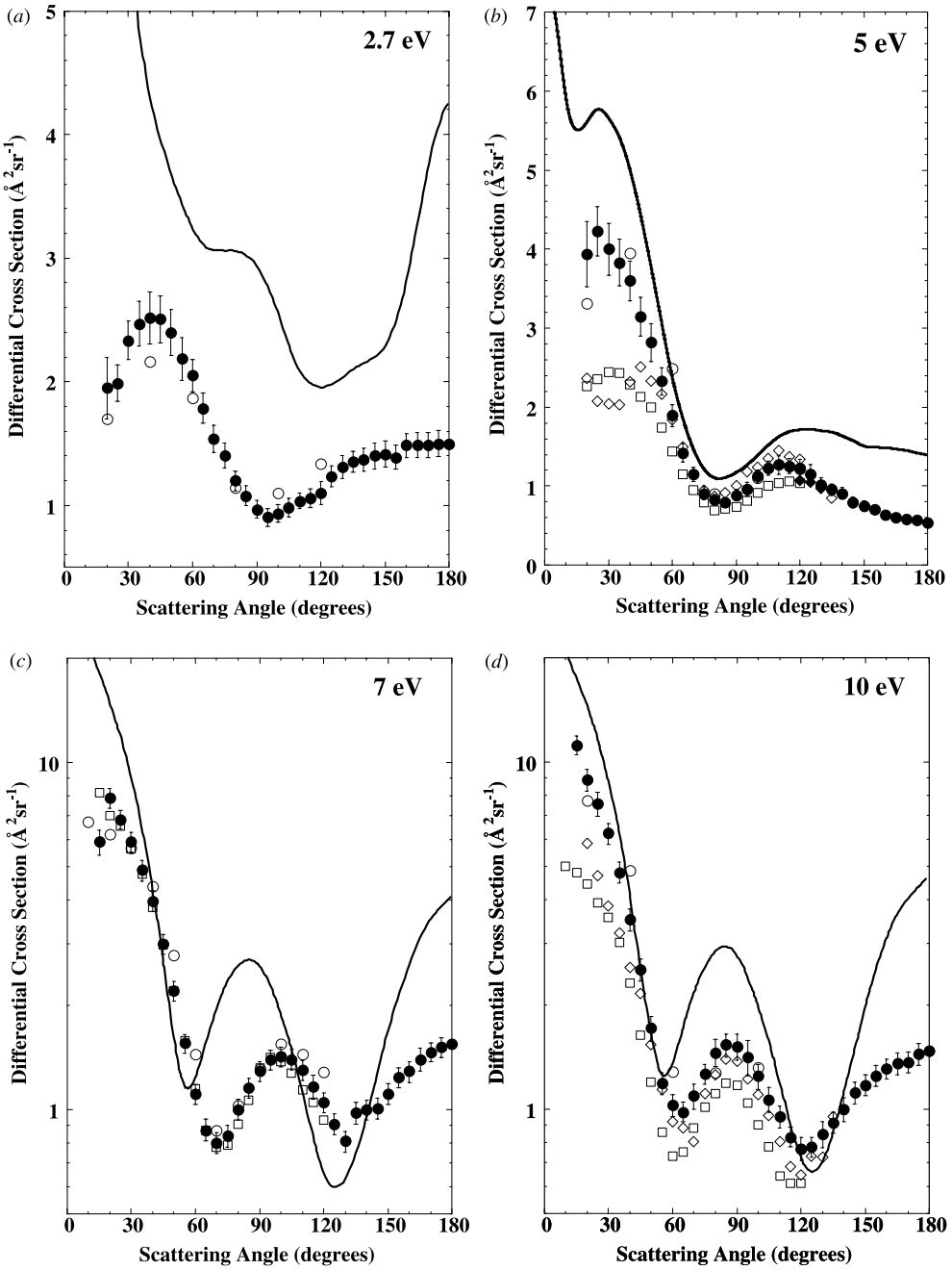

Figure 3. Absolute differential cross section for elastic electron scattering from SF_6 at (*a*) 2.7 eV: ●, present data; ○, Rohr; ——, Gianturco *et al* at 3.3 eV. (*b*) 5.0 eV: ●, present data; □, Johnstone and Newell; ○, Rohr, ◇, Srivastava *et al*; ♦, present 'magnet-on' data in overlapping region; ——, Gianturco *et al*. (*c*) 7.0 eV: ●, present data; □, Johnstone and Newell at 7.2 eV; ○, Rohr; ——, Gianturco *et al* at 10 eV. (*d*) 10 eV: ●, present data; □, Johnstone and Newell, ○, Rohr; ◇, Srivastava *et al*; ——, Gianturco *et al*.

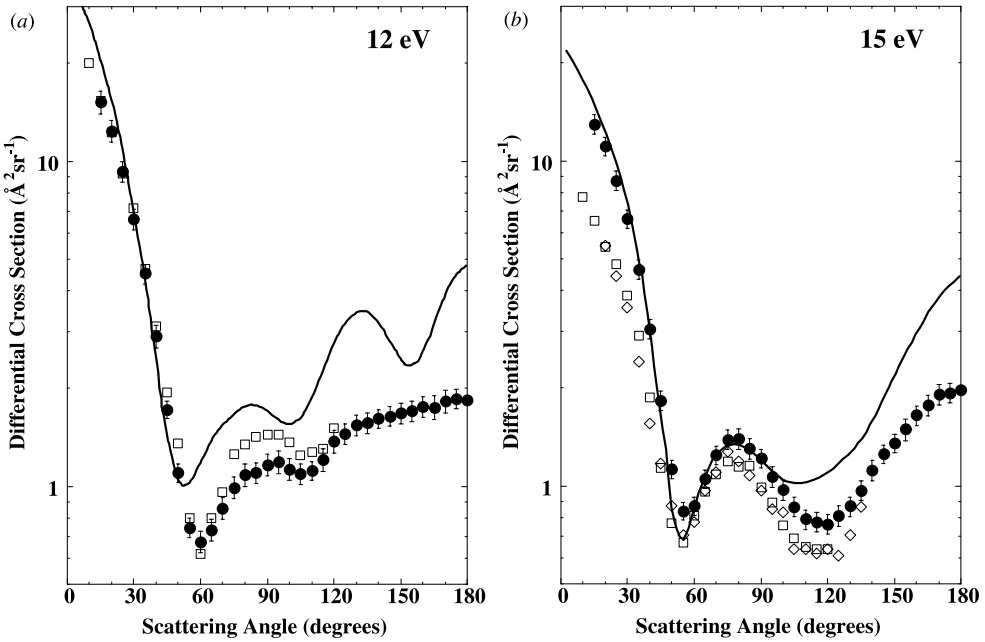

Figure 4. Absolute differential cross section for elastic electron scattering from SF_6 at (*a*) 12 eV: ●, present data; □, Johnstone and Newell; ——, Gianturco *et al* at 13 eV. (*b*) 15 eV: ●, present data; □, Johnstone and Newell; ◇, Srivastava *et al*; ——, Gianturco *et al*.

difference in absolute magnitude between these previous results and the present is almost a factor of two. At larger scattering angles these differences are not quite so dramatic and the present results lie midway between the previous two measurements. On the other hand, there is a dramatic improvement in the level of agreement with the theoretical calculation of Gianturco *et al* at this energy. In the region of overlap, where measurements are taken with and without the magnetic device, the final cross sections shown and tabulated represent an average of all measurements. To indicate the good level of agreement in this overlapping region between the results with and without the magnet, we also show the average values of the measurements taken with the magnet on.

At 7 eV (figure 3(*c*)) all three experimental results agree reasonably well across the entire angular range. Given the differences that are consistently observed at other energies this is somewhat surprising. The DCS shows two minima at 70° and 130° and once again the cross section appears to be *decreasing* for scattering angles of less than about 20°. At backward angles the DCS also appears to be increasing to a local maximum at 180°. A resonance is observed at this energy in the total cross section of Kennerly *et al* (1979) and has also been predicted in the elastic scattering calculations of Dehmer *et al* (1978). The latter work suggests that this resonance, of t_{1u} symmetry, occurs mainly in the $l = 1$ and 3 partial waves. The observed angular distributions do not seem to support this assignment very well, although we note once again that such conclusions must be made cautiously for elastic scattering results, particularly at increasing energies. The calculation of Gianturco *et al* shows the same general features as the experimental results but there are substantial differences both in the magnitude of the cross section and in the position of the maxima and minima. We do not illustrate the cross section at an energy of 8.5 eV as the only measurement available is the present. The angular behaviour, however, is similar to that at 7 eV.

The DCS for an incident energy of 10 eV is shown in figure 3(*d*). The results of Srivastava *et al* and Johnstone and Newell are consistently lower than the present results over the whole angular range and these discrepancies are at their largest at forward angles. The data of Rohr remain in good agreement with the present results at all angles. The level of agreement with the calculation by Gianturco *et al* appears to be improving as the energy is increasing, particularly at smaller scattering angles.

In contrast to all other energies, the present DCS at 12 eV (figure 4(*a*)) is lower in absolute magnitude than that of Johnstone and Newell (1991). This energy corresponds to the position of the large t_{2g} resonance which, according to the calculations of both Dehmer *et al* and Gianturco *et al*, has dominant partial waves of $l = 2, 4$ and 6. The agreement with the calculation of Gianturco *et al* is very good at forward scattering angles. At larger angles, up to 120°, the shape of the cross section is also in good agreement with the theory. However, the present results for backward scattering do not show the large dip in the cross section near 160° which is predicted by theory.

The final graphical comparison that we make is at 15 eV (figure 4(*b*)) which is the highest energy at which the present design of angle-changing magnet can be used. Once again we see that the present measurements are uniformly higher than the two previous cross sections, although the agreement in the shape of the DCS is very good. The agreement between the present cross section and the theoretical calculation is extremely good for scattering angles less than about 90°. At larger angles the agreement in shape is quite good but the present measurement is, for example, about a factor of two lower than the theory at 180°.

We do not show the data at higher energies 20, 30, 50 and 75 eV but similar patterns emerge in a comparison between the available experiments. In general, the present measurements are consistently higher in absolute magnitude than the previous measurements of either Srivastava *et al* or Johnstone and Newell and the theoretical results of Gianturco *et al* agree well with the present data at angles up to 90°. The results at 75 eV have been shown in a previous paper (Cho *et al* 2000) but are of particular interest as they represent the lowest energy in a series of measurements by Sakae *et al* (1989). That comparison demonstrates an excellent level of agreement between the present DCS and that of Sakae *et al* at all scattering angles.

3.2. Total elastic and elastic momentum transfer cross sections

The total elastic cross section σ_i and the elastic momentum transfer cross section σ_m have been derived from the present DCS results by extrapolating to forward and backward angles, where required, and integrating the resultant cross sections. The cross sections resulting from this process are given at the foot of each column in table 1. These results were one of the main motivations for this paper but this aspect of the project has been fully discussed in our earlier communication (Cho *et al* 2000) and the details will not be repeated here.

4. Conclusions

Absolute differential cross sections for elastic scattering of electrons from SF_6 have been measured at 11 energies ranging from 2.7 to 75 eV. In the low-energy region (up to ∼10 eV) the present results show good agreement with the measurements of Rohr (1979). At intermediate energies (5–75 eV) the agreement with two more experimental data sets, those of Srivastava *et al* (1976) and Johnstone and Newell (1991), is rather poor (considerably larger than the combined experimental uncertainties). The largest differences appear to be at more forward scattering angles but there are significant differences across the whole angular range with the present results usually being larger in magnitude than the previous ones. When these are

translated to the integral cross section level the present DCS results in integral elastic cross sections which are substantially larger than the earlier results of Srivastava *et al* and Johnstone and Newell. The agreement with the theory of Gianturco *et al* (1995) is rather poor at low energies but improves markedly as the energy is increased, particularly at lower scattering angles. At the energy where they overlap, at 75 eV, the present data show good agreement with those of Sakae *et al* (1989).

In these measurements, an electron-beam deflecting magnet has successfully been used with the relative flow technique to measure absolute differential cross sections for the backward hemisphere. We are of the opinion that this innovative technique of the Manchester group will prove to be of great benefit in the future in the study of short-range interactions which are generally more important at larger scattering angles and in the more accurate derivation of integral cross sections.

Acknowledgments

Stimulating discussions with James Olthoff and Loucas Christophorou, who encouraged us to perform these measurements, are gratefully acknowledged. HC gratefully acknowledges the award of an Australian Research Council (ARC) International Visiting Fellowship, RJG an ARC Postdoctoral Fellowship and LJU an Australian Government Postgraduate Award (APA). We are grateful to the technical staff of the Atomic and Molecular Physics Laboratories, particularly Steve Battisson and Kevin Roberts, for their expert assistance.

References

Allan M 2000 *J. Phys. B: At. Mol. Opt. Phys.* **33** L215
Brunger M J, Buckman S J, Allen L J, McCarthy I E and Ratnavelu K 1992 *J. Phys. B: At. Mol. Opt. Phys.* **25** 1823
Brunger M J, Buckman S J and Newman D S 1990 *Aust. J. Phys.* **43** 665
Brunt J N H, King G C and Read F H 1977 *J. Phys. B: At. Mol. Phys.* **10** 1289
Buckman S J, Gulley R J, Moghbelalhossein M and Bennett S J 1993 *Meas. Sci. Technol.* **4** 1143
Cho H, Gulley R J and Buckman S J 2000 *J. Phys. B: At. Mol. Opt. Phys.* **33** L309
Christophorou L G, Olthoff J, Siegel R, Hayashi M and Nakamura Y 1999 *Bull. Am. Phys. Soc.* **44** 20
Christophorou L G and Van Brunt R J 1995 *IEEE Trans. Dielectr. Electr. Insul.* **2** 952
Dababneh M S, Hsieh Y-F, Kauppila W E, Kwan C K, Smith S J, Stein T S and Uddin M N 1988 *Phys. Rev.* A **38** 1207
Dehmer J L, Siegel J and Dill D 1978 *J. Chem. Phys.* **69** 5205
Ferch J, Raith W and Schröder K 1982 *J. Phys. B: At. Mol. Phys.* **15** L175
Fursa D V and Bray I 1997 *J. Phys. B: At. Mol. Opt. Phys.* **30** 757
Gianturco F A, Lucchese R R and Sanna N 1995 *J. Chem. Phys.* **102** 5743
Gibson J C, Green M A, Trantham K W, Buckman S J, Teubner P J O and Brunger M J 1999 *J. Phys. B: At. Mol. Opt. Phys.* **32** 213
Gibson J C, Morgan L A, Gulley R J, Brunger M J and Buckman S J 1996 *J. Phys. B: At. Mol. Opt. Phys.* **29** 3197
Gulley R J, Alle D T, Brennan M J, Brunger M J and Buckman S J 1994 *J. Phys. B: At. Mol. Opt. Phys.* **27** 2593
Gyemant I, Varga Z S and Benedict M G 1980 *Int. J. Quantum Chem.* **17** 255
Hayashi M and Nimura T 1984 *J. Phys. D: Appl. Phys.* **17** 2215
Jansen R H, de Heer F J, Luyken H J, van Wingerden B and Blaauw H J 1976 *J. Phys. B: At. Mol. Phys.* **9** 185
Jiang Y, Sun J and Wan L 1995 *Phys. Rev.* A **52** 398
——1997 *Phys. Lett.* A **231** 231
Johnstone W M and Newell W R 1991 *J. Phys. B: At. Mol. Opt. Phys.* **24** 473
Kasperski G, Mozejko P and Szmytkowski C 1997 *Z. Phys.* D **42** 187
Kennerly R E, Bonham R A and McMillan M 1979 *J. Chem. Phys.* **70** 2039
Landolt-Börnstein 1971 *Zahlenwerte und Funktionen* vol 2, part 1 (Berlin: Springer)
McConkey J W and Preston J A 1975 *J. Phys. B: At. Mol. Phys.* **8** 63
Nesbet R K 1979 *Phys. Rev.* A **20** 58

Nickel J C, Zetner P W, Shen G and Trajmar S 1989 *J. Phys. E: Sci. Instrum.* **22** 730
Read F H and Channing J M 1996 *Rev. Sci. Instrum.* **67** 2372
Register D F, Trajmar S and Srivastava S K 1980 *Phys. Rev.* A **21** 1134
Reid R C, Prausnitz J M and Poling B E 1987 *The Properties of Gases and Liquids* (New York: McGraw-Hill)
Rohr K 1977 *J. Phys. B: At. Mol. Phys.* **10** 2215
——1979 *J. Phys. B: At. Mol. Phys.* **12** L185
Sakae T, Sumiyoshi S, Murakami E, Matsumoto Y, Ishibashi K and Katase A 1989 *J. Phys. B: At. Mol. Opt. Phys.* **22** 1385
Srivastava S K, Chutjian A and Trajmar S 1975 *J. Chem. Phys.* **63** 2659
Srivastava S K, Trajmar S, Chutjian A and Williams W 1976 *J. Chem. Phys.* **64** 2767
Trajmar S and Chutjian A 1977 *J. Phys. B: At. Mol. Phys.* **10** 2943
Trajmar S, Register D F and Chutjian A 1983 *Phys. Rep.* **97** 216
Trantham K T, Dedman C J, Gibson J C and Buckman S J 1997 *Bull. Am. Phys. Soc.* **42** 1727
Wilhelm E and Battino R 1971 *J. Chem. Phys.* **55** 4012
Zecca A, Karwasz G and Brusa R S 1992 *Chem. Phys. Lett.* **199** 423
Zubek M, Gulley N, King G C and Read F H 1996 *J. Phys. B: At. Mol. Opt. Phys.* **29** L239
Zubek M, Mielewska B, Channing J, King G C and Read F H 1999 *J. Phys. B: At. Mol. Opt. Phys.* **32** 1351